JPSE (Journal of Physical Science and Engineering), Vol. 4, No. 2, 2020, Page 74–83
DOI: 10.17977/um024v4i22019p074

JPSE
(Journal of Physical Science and Engineering)

http://journal2.um.ac.id/index.php/jpse
EISSN: 2541-2485

The External Electric Field Effect to Hydrogen Storage on B-N Co-Doped Graphene Surface Decorated by Metal Atoms: A DFT Study

Received
15 May 2020

Revised
08 July 2020

Accepted for Publication
17 July 2020

Published
25 August 2020

A Sarmada* **and S Pupon**

Graphica Engineering, Politeknik Negeri Media Kreatif, Srengseng Sawah Street, Jagaksara, South Jakarta, 12640, Indonesia.

***Email:** asarmada007@gmail.com

Abstract
Hydrogen has been concerned to be ideal clean energy. However, some challenges have to be addressed before hydrogen will become an available energy carrier. For instance, the volumetric energy of hydrogen has an issue such as controlling in ambient conditions with reliable utilities. Recently, carbon based materials such as graphene and carbon nanotubes have been designed for hydrogen storage due to their large surface area, lightweight, and tunable properties. Controlling the binding strength of metal atoms with that of the boron (B) and nitrogen (N) co-doped graphene (BNDG) surface is an essential issue in applying hydrogen storage. Recent studies have shown that the bonding strength between the metal atom and the substrate can be controlled using an external electric field. In this study, we have considered BNDG and investigated its hydrogen storage capacity by decorating different metal atoms. We utilize the DFT calculations study to investigate the hydrogen storage properties materials. By applying an external electric field on the Ti_3 decorated BNDG sheet, we have demonstrated that the adsorption energy of H_2 molecules can increase substantially and thereby tune the overall hydrogen storage capacity.
Keywords: DFT, graphene, boron nitrogen doped, hydrogen storage, electric field effect.

1. Introduction

Decorated doped carbon based materials are essential for the chemical fuel industry due to their electronics properties and unique material instability storage for gas fuels. These carbon based materials usually refer to graphene derivatives, such as graphene (2D-sp3 carbon structure of hydrogenated graphene), graphene foam (GFs), graphene oxide, acetylenic graphene, fluorographene, fullerene, carbon nanotubes (CNTs), and boron doped graphene [1].

Energy storage technologies are critical in addressing the global challenge of clean sustainable energy. It is well recognized that the development of high energy storage devices is vital to help diversify our energy resources and reduce our dependency on fossil fuels. Introducing boron doped by substituting boron in graphenes structure, electronics properties within the carbon-carbon bond of graphene are changing by increasing shift of G-band, meanwhile increasing boron doped concentration makes the graphene become more like semiconductor (p-type). Besides, the decorating graphene by metal show improvement for proper adsorption and desorption site for H_2 gas molecule, e.g. increasing maximum capacity and H_2 coverage in graphene (by transition metal decorating) is commonly in use and necessary to keep H_2 storage that required by DOE target of 9 wt% in 2020 [2].

The beginning of H_2 storage materials is already right in approaching storage capacity. The release of hydrogen is also the key to the usage of hydrogen fuels. The challenging for new generation fuels have materials that are good potential for adsorbing H_2 gas and quickly releasing hydrogen after stored for some time which offering instantaneous hydrogen releasing [3].

Boron and nitrogen doped graphene. In recent years, graphene has been well known because of its large surface area, high porosity, excellent thermal and electrical conductivities, and the most important is very thin-strong nanosheets [4]. Since the invention of graphene, it plays an essential role in hydrogen adsorption that has lightweight as a fuel tank. Consequently, the payload of weight can be reduced and a higher amount of hydrogen capacity can be achieved in this stable state. For a real application, many researchers are now developing high absorptivity of graphene therefore it could be applicable as real hydrogen fueled vehicles. Besides, it has a robust structure which can be applied under high compression of hydrogen [5]. To get better performance of graphene in hydrogen storage materials, this graphene requires to be modified by doping materials such as boron, nitrogen, and another element [6], [7].

This modification will improve characteristics and stability during the use of graphene as support for the hydrogen storage system. The idea is available by carbon doping on the boron nitride (B-N) sheet, and the other ways are B-N doping on carbonaceous graphene. Some cases of them show the unstable doping due to atomic dislocation on boron doping [8]. Related to the concentration of doping, the B-N co-doping graphene becomes more critical than carbon doping B-N sheets due to a lower level of B-N than carbon on the system. Nevertheless, the characteristics offered to be enhanced by boron doped increases the binding energy between adsorbed metal and graphene support. While nitrogen doping can support the deficiency of electron in boron doped graphene, it also sustains the increase of boron concentration in grapheme. Therefore, more full area of distribution is promised in boron and nitrogen doping materials. Boron and nitrogen doped graphene have been the most intensively developed in the doping system because boron has three valences (lack of an electron from carbon) and nitrogen has five valences (gained an electron from carbon). Therefore, boron and nitrogen can open up a possibility to be a neighbouring element in graphene system [9].

The demand for hydrogen fuels is concentrated on replacing fossil fuels that conventionally used for a long time ago. The hydrogen fuels are the most concentrated solution on the environmental issue because the side products of hydrogen fuels are remarkably safe. Yet, the hydrogen fuel remains a problem that required the systems for concentration and storage. Although hydrogen is natural to be synthesized by water splitting and methane reforming process, the hydrogen gas needed to be concentrated on storage materials to get high energy density in gravimetric and volumetric [10].

The importance of hydrogen storage materials research is to analyze the binding mechanism of H_2. Antibonding of hydrogen has never been used in most of the way of binding mechanism. It is because the electrons that spend most of their time between the nuclei of two atoms are placed into the bonding orbitals. Electrons that contribute most of their time outside the nuclei of two atoms are placed into antibonding orbitals and cause an increase in electron density between the nuclei in bonding orbitals, and a decrease in electron density in antibonding orbitals [11]. In vice versa, if the binding mechanism placed on the antibonding orbitals, there is an increase in electron density in antibonding orbitals and a decrease in electron density in between the nuclei in bonding orbitals.

The external electric field creates excess surface charge which can manipulate the adsorption rate on the substrate by the enhanced electrostatic interactions between the electrode and gas molecule by coupling with complementary charges. The higher electric field could influence the conformation and similar properties such as direct electrochemistry and surface character [12]. However, a high external electric field leads to damage of the surface sites. This is corresponding to defect sites increment and reduces the stability of surface support. The external electric field can help to modulate the surface charge and then the surface can make contact with adsorbed gas on the material surface via electrostatic force [13].

In the approach presented in this study, we utilize the DFT calculations study to start a study about investigating the hydrogen storage properties materials. Initially, we begin with a unit cell graphene structure which consists of four carbon atoms and placed in a 15 Å vacuum of the slab. The second step would be to supercell the size of a unit cell into a triplication cell and change four atoms of carbon into boron atoms and four atoms another into nitrogen atoms. One ring of graphene should have at least one atom of boron and one atom of nitrogen. The boron and nitrogen atoms can be isomerization in the near neighbouring side and inter distance side. By this study, the characteristic of the adsorbed molecular hydrogen on the B-N co-doped graphene affected by external electric field can be explored.

2. Method

2.1. Design of the Research

All calculations have been carried out using density functional theory (DFT) as implemented in the ab initio simulation package. The exchange correlation energy was calculated within the generalized gradient approximation (GGA) [14], [15] with the use of the Perdew-Wang functional [16]. The projector augmented wave method implemented in VASP was applied [17]. The Brillouin zone was sampled with a Monkhorst-Pack grid, and the k-point was performed with (6 × 6 × 1) in our calculations. A cut off the energy of 430 eV was used to make the plane wave basis set finite and a hexagonal supercell with a dimension of (14.81 × 12.84 × 29.87) $Å^3$ included a p-(3 × 2) unit cell with periodic boundary conditions was used for metal decorated B-N co-doped graphene surface. The conjugate gradient method was used in ionic relaxations until the forces on all unconstrained atoms were less than 1×10^{-2} eV/Å. Spin polarization has been applied in all calculation.

Here, the adsorption energy was defined as follow

$$E_{ads} = E_{total} - E_{surface} - E_{adsorbate} \tag{1}$$

where E_{total} is the total energy of the system, $E_{adsorbate}$ is the calculated energy of a molecule in the gas phase, and $E_{surface}$ is the energy of the surface. $E_{ads} < 0$ corresponds to favourable or exothermic adsorption of molecules on the surface.

In related with the adsorbate was a trimetallic M_3 on the graphene surface, the binding energy of metal to graphene surface was denoted as adsorption energy E_{ads}. By this definition, the metal consists of ligand bonding energy to metal cluster and contact with the graphene surface. In the term to defined the metal binding energy, the adsorption energy of metal was also considering metallic bonds energy that involved between metal to metal binding energy and metal to graphene binding energy.

For metal to metal binding energy (in eV/atom), the energy was calculated by the following equation

$$E_{bind}^{M-M} = \left(\frac{E_{total} - E_{surface} - n \times E_{M1}}{n} \right) \tag{2}$$

for trimetallic to surface graphene, the energy (in eV/atom) was calculated by the following equation

$$E_{bind}^{M-M} = \left(\frac{E_{total} - E_{surface} - E_{M3}}{3} \right) \tag{3}$$

The total adsorption energy of H_2 was defined as the following equation

$$E_{ads-Tot} = E_{total} - E_{surface} - nE_{H_2} \tag{4}$$

and the average adsorption energy for hydrogen was defined as follows

$$E_{ads-H_2} = \left(\frac{E_{total} - E_{surface} - nE_{H_2}}{n} \right) \tag{5}$$

where E_{total} is the total energy of the system, $E_{surface}$ is the energy of the surface, E_{H_2} is the calculated energy of hydrogen molecule in the gas phase, and n is the number of adsorbed hydrogen. $E_{ads-H_2} < 0$ corresponds to favourable or exothermic adsorption of molecules on the surface.

In addition, stepwise energy for hydrogen was also defined as follow

$$(n)E_{stepwirse} = E_{ads-H}(n) - E_{ads-H}(n-1) \tag{6}$$

Here $E_{ads-H}(n)$ is the adsorption energy of (n) hydrogen atom, and $E_{ads-H}(n-1)$ is the adsorption energy of $(n-1)$ hydrogen atom. $(n)E_{stepwirse} > 0$ means that it is unfavorable to add $(n)^{th}$ hydrogen atom.

2.2. Procedure and Data Collection

The M_3 decorated on B-N co-doped graphene surface we used was performed by our previous work on B doped graphene [18]. First, we calculated a single layer of carbon in a hexagonal lattice by PAW method and its bulk lattice constant was 2.46Å, which was in agreement with the experimental results [19]. Second, we tried to demonstrate the effect after doping boron nitride. According to previous experimental results [20], the low concentration of boron is thought to be randomly substituted for carbon. Third, we did the benchmark of Pt adsorption. We found that Pt adsorption energy has a very small change in the different cut off energy and k-points. Therefore, we choose the energy cut-off of 430 eV and (5 × 5 × 1) k-point which have better calculate performance as our calculated setting. Finally, we performed the deposition configurations of the trimetallic cluster of M_3 on (3 × 3) graphene adsorption sites of the B-N co-doped graphene. As the result, the metal particles did not prefer to form a cluster of several types of metal on B-N co-doped graphene surface due to the strong interaction between the metal and graphene layers.

The available configurations of M_3 B-N co-doped graphene in uniform 34% doped concentration are hollow, top, and bridge. Here is the comparison of energy binding and total energy of M_3 B-N co-doped grapheme, as seen in Table 1. The highest binding energy from the table is Sc with -1.46 eV/atom binding energy, but the Sc_3 cluster has low activity in H_2 adsorption. Then, the 2nd highest binding energy is Ti with -1.22 eV/atom and also has highest activity in H_2 adsorption.

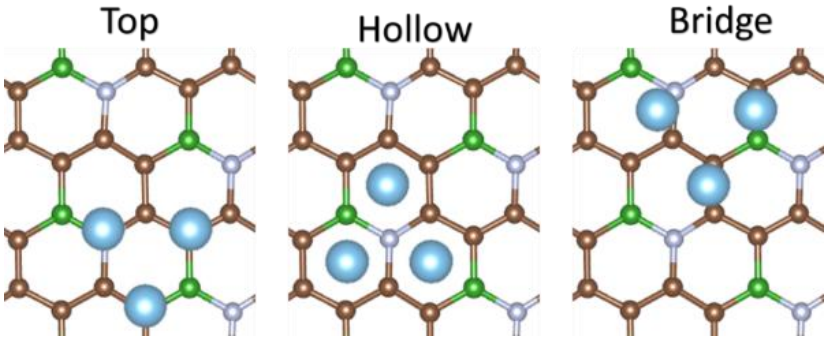

Figure 1. Top and side view of the M_3 B-N co-doped graphene surface.

Table 1. Comparison of energy binding and total energy of M_3 B-N co-doped graphene.

System	Total Energy (eV)			Binding Energy (eV/atom)		
	Hollow	**Top**	**Bridge**	**Hollow**	**Top**	**Bridge**
Mg	-	-	-211.42	-	-	-0.13
K*	-213.85	-	-	-0.93	-	-
Ca*	-	-	-213.43	-	-	-0.63
Sc	-225.14	-224.18	-	-1.46	-1.14	-
Ti	-227.36	-227.29	-	-1.22	-1.20	-
V	-228.41	-229.85	-	-0.41	-0.89	-
Cr	-	-	-230.27	-	-	-0.24
Mn	-229.84	-229.12	-	-0.78	-0.54	-
Fe	-	-227.15	-	-	-0.52	-
Co	-	-	-223.33	-	-	-0.58
Ni	-219.39	-	-219.30	-0.47	-	-0.44
Cu	-215.56	-	-	-0.23	-	-
Zn	-	-211.31	-	-	-0.19	-
Ge	-	-	-219.53	-	-	-0.02

3. Result and Discussion

Boron doped and nitrogen doped graphene have different characterizations in electronic structure. Both dopant atom is important due to unique properties in the bandgap and relative surface stabilization energy. For deep evaluation of the relative stability of B, N-codoped-sheet, we will use the concept of formation energy ($\triangle E_{form}$) defined as

$$\Delta E_{form} = E_{Total}(C_x N_y B_z) - \frac{x}{n_{tot}} \times E(C) - \frac{y}{n_{tot}} \times E(N) - \frac{z}{n_{tot}} \times E(B) \quad (7)$$

where $E_{Total}(C_x N_y B_z)$, $E(C_x)$, $E(N_y)$, and $E(B_z)$ are the energy of total system energy carbon, nitrogen, and boron potential energy. The potential energy of carbon, nitrogen, and boron has been carried out based on empirical potential from bulk graphite, nitrogen gas, borane gas respectively.

Based on our calculation, as seen in Table 2, the concentration of B-N co-doped graphene reached 25.00% to 33.33% is the most favorable concentration to doping B-N on graphene surface due to low formation energy. Therefore, these studies are choosing 33.33% concentration due to a uniform doped pattern. The doping concentration list energy showed that 25.00% to 33.33% is the optimum stable concentration for graphene to be co-doped by B-N atom.

3.1. Metal Adsorption on BNDG

The binding energy of a trimetal atom of the transitional group nearby a B-N co-doped graphene site is investigated using the DFT method. The optimized structure of B-N co-doped graphene was found in the planar monolayer before metal decoration. After metal decoration, the planar monolayer graphene was defected by trimetal atom and become waved graphene. The optimization of B-N co-doped graphene was done by (6 × 6) multiplication of graphene unit cell. Previously, the smaller size of the graphene slab has not pretended a characteristic of waved graphene (Figure 2). The benchmarking slab size was done in various sizes of the unit cell (Table 3).

First, we consider the binding energy of trimetal decoration to B-N co-doped graphene system with Mg, K, Ca, Sc, Ti, V, Cr, Mn, Fe, Co, Ni, Cu, Zn, and Ge. The choice of metals is selecting all metal with lightweight categorize metal and all transitional metal in 4th row. The basic concept of hydrogen storage materials using lightweight supported metal to reduce the weight percentage of metal to the overall system, then the weight capacity of H_2 could increase for a system with the same H_2 molecules amount. These H_2 molecules recently have been demonstrated physisorption and chemisorption on metal as well as in defected graphene, while the chemisorption is not preferable to be desorbed than physisorption's one. The configuration of this adsorption is related to H_2 adsorption energy. The H_2 adsorption is latter needed to be also considered in metal selection so the adsorption type of H_2 could be controllable for adsorption or desorption. The second consideration of metal selection is the first H_2 molecules adsorption energy. This first adsorption energy will also determine how much high the latter adsorption of H_2 molecules.

Table 2. Formation energy of different concentration of B-N co-doped graphene.

Concentration (%)	Total Energy (eV)	$\triangle E_{form}$ (eV)	Relative E_{form} (eV)
0.00	-221.57	-8.85	0.00
8.33	-209.44	-8.35	0.50
16.67	-202.84	-8.08	0.77
25.00	-212.04	-8.47	0.37
33.33	-210.37	-8.41	0.44
33.33*	-202.17	-8.07	0.78
50.00	-195.57	-7.81	1.04
58.33	-194.90	-7.79	1.06
75.00	-202.61	-8.13	0.72
100.00	-210.39	-8.47	0.37

*This type of doping is in non-uniform pattern

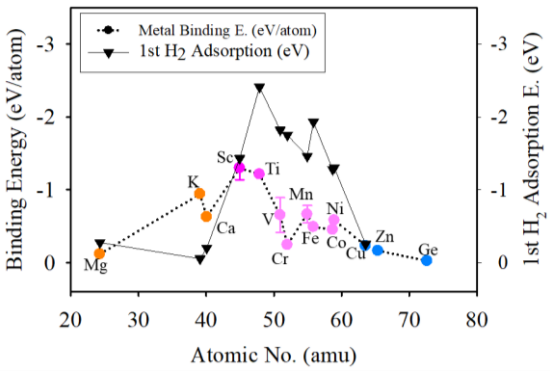

Figure 2. Comparison of E_{bind}^{M-G} (circle dot) and E_{H2} (triangle) in various metal on B-N co-doped graphene.

Table 3. List of structure parameter comparison in double sided structures and single sided.

Type	Total E (eV)	Magnetic mo. (μB)	E Bind (eV/atom)	d (Ti–G) (Å)	
				Top	Lower
1 (Top, hollow)	-243.90	2.48	-1.15	2.15	1.86
2 (Top, top)	-244.80	4.00	-1.30	2.13	2.14
3 (Top, hollow)	-243.89	5.94	-1.14	2.16	1.83
4 (Top, top)	-244.12	3.28	-1.19	2.17	2.25
5 (Hollow, hollow)	-244.23	6.00	-1.20	1.79	1.87
Single sided (hollow)	-227.36	1.44	-1.22	1.84	1.84
Single sided (top)	-227.29	2.00	-1.20	2.15	2.15
Ti-N ref [22]			-1.10		

Titanium metal was the highest binding energy of metal decoration in B-N co-doped-graphene, it prefers to be more adsorbed in surface compare to another metal. By the mean, the titanium cluster has the most stable binding energy with B-N co-doped surface.

Another way to select a metal decoration system on hydrogen storage materials is considered the first H_2 adsorption energy. It is important to check whether the metal decoration can adsorb and also desorb hydrogen molecules during the storing process. In contrast, we are plotting the energy adsorption of trimetallic on B-N co-doped graphene and first H_2 adsorption energy of each trimetallic system. The result was plotted in Figure 2. From Figure 2, the metal which has the potential to be decorated at B-N co-doped graphene were Ti and V due to higher binding energy of metal to graphene. In case of the application of a metal decorated system that will produce in mass production. The MD result showed that Ti and V can be stabilized on B-N co-doped graphene surface.

The trend line of metal adsorption on B-N co-doped graphene was comparable with the experimental result of Ti-N XPS spectra that showed 2p Ti orbital was bounded to 1s N orbital with binding energy around 1.1 eV [21]. Other references that involved transitional metal binding energy with carbon based material showed the different value of binding energy. The binding energies were up to 4–5 eV showed in this reference, that's due to single atomic decorated. It was believed that trimer is more following and reliable in the experimental result than single atomic decoration. Antibonding orbital near Fermi level of Ti decorated B-N co-doped graphene showed the contribution s-orbital antibonding was predominant on the first peak Ti, on the other hand, V d-orbital looks like more dominance than its s-orbital. Furthermore, the s-orbital of Ti antibonding orbital showed more polarizable than V on the following figure due to single peak versus double peak within an opposite spin.

3.2. Double Side Decoration

Double-sided decoration of Ti_3 on B-N co-doped graphene was being optimized to find the most stable structure. These empirically optimized structures considered the top and hollow site of Ti_3 in B-N co-doped graphene and confirm the minimum polarizability within the lowest energy minimum. Here are the list and the details of the structure as seen in Table 3.

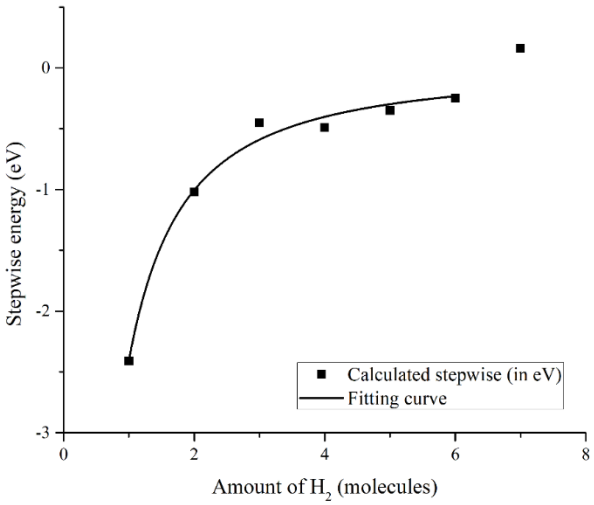

Figure 3. Total adsorption energy for each H_2 adsorption on Ti_3 cluster.

The metal binding energy and magnetic moment were observed in double-sided and had a tendency to be increased. The most stable structure for Ti_3 on single-sided decoration is in the hollow site of B-N co-doped graphene. The double-sided was observed that top site was the lowest energy minimum's position. These changes due to increasing of magnetization on metal. The type of hollow-hollow site of Ti_3 double decoration has an advantage for the highest magnetization activity to help the hydrogen adsorption that involved magnetized adsorption.

3.3. Adsorption of Molecular Hydrogen

The adsorption of H_2 on Ti_3 was observed by step by step adsorption H_2 molecule on Ti_3 cluster. The first and the second adsorption was form chemisorption and followed by physisorption then. As the coverage increases, the stepwise adsorption energies decrease showing in the below table and figure. The eighth adsorption showed positive stepwise energy, which means the stability of H_2 metal does not exist. The maximum adsorption up to seven molecules of H_2 in Ti_3 cluster is favorable thermodynamically as indicated by this stepwise adsorption energy. The chemisorbed H_2 has also been shown to have a large decrement on second stepwise energy as seen in Figure 3.

3.4. Effects of Electric Field on Metal Binding

The electric field was proposed to see controllable hydrogen adsorption strength on metal decorated on B-N co-doped graphene. This electric field is a property that describes the space that surrounds electrically charged particles. Free metal clusters have a size dependent charge and it's nonscalable for nanoclusters. Decorated nanocluster of Ti_3 on B-N co-doped graphene was also forming positively and negatively charged clusters. Therefore, the neutral system was used to investigate the presence of the electric field.

By nomenclature, it advised to increase and decrease the electric field so the adsorption energy of hydrogen molecule can be controlled by switch electric field. It supposed the increasing electric field can increase the charge transfer from the surface to the hydrogen molecule. However, the remained problem occurred when the metal stability before applying the electric field on the surface was questioned, how much charge can be gathered by a small tip of a metal decorated system. To answer this question, the metal stabilities were checked before the adsorption of hydrogen molecules. Being more advanced in mental stability, three types of metals, titanium, nickel, and manganese were prepared well in decorating the M_3 (trimetallic) system on B-N co-doped graphene and their charge was got by optimization at the neutralized system. Each energy of applied electric field on the system was carried on a calculation of single point energy

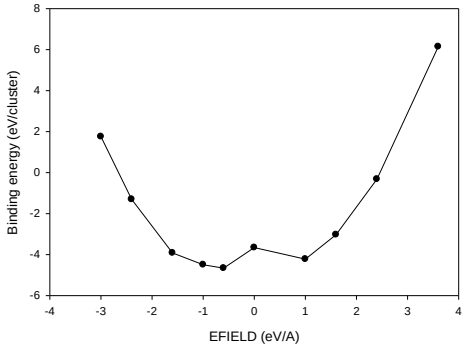

Figure 4. Metal stability on cluster binding energy by effect of electric field on z-direction.

The binding energy was obtained from two different formulas as below

$$E_{bind} = E^{F}_{BN/M_3} - E^{F}_{BN} - E^{0}_{M_3} \quad (8)$$

$$E_{bind} = E^{F}_{BN/M_3} - E^{F}_{BN} - E^{F}_{M_3} \quad (9)$$

Noted, it was represented binding energy between metal and B-N co-doped graphene and were total energy of metal decorated in B-N co-doped graphene, the surface energy of B-N co-doped graphene, and trimetallic system alone respectively. The superscript of introducing as a system with an applied electric field. Therefore, here is the result of calculation metal stability in the applied electric field on the system as seen in Figure 4. The electric field effect gives limiting value due to metal binding energy to 0.4 eV. The binding energy of metal becomes repulsive in an increment of 0.6 and 0.8. The maximum charge was well redistributed in 0.4 eV and then decreasing, as seen in Figure 4.

The electric field effect was given as a switch for H_2 storage. A switch is often used in adsorption for introducing distributed charges on the surface which enhanced the adsorption energy during storage. Based on the study of metal selection, Ti_3 was the first metal for the adsorption part, so the increasing behavior of the electric field becomes the primary parameter for Ti_3 to adsorb more hydrogen on the system. Hereby, this study was concern about H_2 adsorption energy in the Ti_3 cluster. In the case of the Ti_3 adsorption part, the effect of the electric field (Figure 5).

The spillover, those effects in the especially hydrogen storage system and active particles in heterogeneous systems allowed the flowing of an H particle from a decorated metal activator (donor) to the graphene surface carrier (acceptor). These heterogeneous systems are mainly transitional metal ones, where this interesting effect has been observed in this study pass through electric field effect. The effect has attracted considerable interest when the mechanism of heterogeneous thermal and photo processes on the so called deposited titanium trimetal clusters (Ti_3) was studied in B-N co-doped graphene that successfully synthesized in the real application and those had beneficially used due to high surface coverage area and stability in full dispersion to promote high active site efficiency as hydrogen activator for H_2 storage systems by spillover method. The electric field has been proved to enhance the H_2 adsorption energy and metal binding energy due to more distribution of charge during adsorption, as seen in Figure 5.

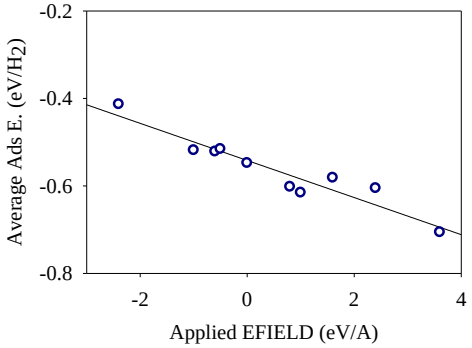

Figure 5. Electric field effect on H_2 adsorption energy at Ti_3 from -2.4 to 3.6 eV/Å.

4. Conclusion

The hydrogen storage capacity on both single and double-sided different metal atoms decorated on the boron-nitrogen co-doped graphene (BNDG) sheet has been investigated using first principles calculations. Among the different metals, the Ti, V, and Sc have the larger binding energy of -1.22, -0.89, and -1.14 eV/atom, respectively on B, N, co-doped graphene surface. The molecular dynamic simulations indicate that V and Ti atoms are uniformly dispersed on the BNDG sheet without clustering and it has good thermal stability even at a higher temperature (400K). Furthermore, it is found that the single- sided Ti_3 decorated BNDG sheet can hold up to seven H_2 molecules with an average hydrogen adsorption energy of -0.52 eV. By applying an external electric field on the Ti_3 decorated BNDG sheet, we have demonstrated that the adsorption energy of H_2 molecules can increase substantially and thereby tune the overall hydrogen storage capacity. These theoretical predictions can serve as a guiding reference to experimental works in developing efficient hydrogen storage materials for practical implementations.

Reference

[1] N. Mahmood *et al.*, "Graphene based Nanocomposites for Energy Storage and Conversion in Lithium Batteries, Supercapacitors, and Fuel Cells," J. Mater. Chem. A., vol. 2, no. 1, pp. 15–32, 2014.

[2] K. L. Lim *et al.*, "Solid State Materials and Methods for Hydrogen Storage: A Critical Review," *Chem. Eng. Technol.: Indust. Chem. Plant Equipment-Process Eng.-Biotechnol.*, vol. 33, no. 2, pp. 213–226, 2010.

[3] P. Hoffmann, *A History of Hydrogen Energy: A BIT of Tomorrow's Energy*, Massachusetts: MIT Press, 2014.

[4] D. Moitra *et al.*, "Synthesis and Microwave Absorption Properties of $BiFeO_3$ Nanowire-RGO Nanocomposite and First Principles Calculations for Insight of Electromagnetic Properties and Electronic Structures," *J. Phys. Chem. C.*, vol. 121, no. 39, pp. 21290–21304, 2017.

[5] A. B. Julia *et al.*, "Mechanical Properties of Crumpled Graphene under Hydrostatic and Uniaxial Compression," *J. Phys. D: Appl. Phys.*, vol. 48, no. 9, p. 095302, 2015.

[6] Y. Wang *et al.*, "Materials, Technological Status, and Fundamentals of PEM Fuel Cells–A Review," *Materials Today*, vol. 32, pp. 178–203, 2019.

[7] O. Gohardani, M. C. Elola, and C. Elizetxea, "Potential and Prospective Implementation of Carbon Nanotubes on Next Generation Aircraft and Space Vehicles: A Review of Current and Expected Applications in Aerospace Sciences," *Progress in Aerospace Sci.*, vol. 70, pp. 42–68, 2014.

[8] R. A. C. Castillo, M. E. Law, and K. S. Jones, "Impact of Dopant Profiles on the End of Range Defects for Low Energy Germanium Preamorphized Silicon," *Materials Sci. Eng. B.*, vol. 114, pp. 312–317, 2004.

[9] H. Deng *et al.*, "Active Sites for Oxygen Reduction Reaction on Nitrogen Doped Carbon Nanotubes derived from Polyaniline," *Carbon*, vol. 112, pp. 219–229, 2017.

[10] A. M. Abdalla *et al.*, "Hydrogen Production, Storage, Transportation, and Key Challenges with Applications: A Review," *Energy Conv. Manag.*, 165, pp. 602–627, 2018.

[11] M. M. Morgan, "Boron-Nitrogen Analogues of Indene Containing Hydrocarbons," Ph.D. dissertation, Department of Chemistry, Faculty of Graduate Studies, University of Calgary, Alberta, 2019.

[12] A. Vilan and D. Cahen, "Chemical Modification of Semiconductor Surfaces for Molecular Electronics," *Chem. Rev.*, vol. 117, no. 5, pp. 4624–4666, 2017.

[13] V. Lee *et al.*, "Collisional Charging of Individual Submillimeter Particles: Using Ultrasonic Levitation to Initiate and Track Charge Transfer," *Phys. Rev. Materials*, vol. 2, no. 3, p. 035602, 2018.

[14] J. P. Perdew *et al.*, "Atoms, Molecules, Solids, and Surfaces: Applications of the Generalized Gradient Approximation for Exchange and Correlation," *Phys. Rev. B.*, vol. 46, no. 11, pp. 6671–6687, 1992.

[15] J. P. Perdew and W. Yue, "Accurate and Simple Density Functional for the Electronic Exchange Energy: Generalized Gradient Approximation," *Phys. Rev. B.*, vol. 33, no. 12, pp. 8800–8802, 1986.

[16] J. P. Perdew and Y. Wang, "Accurate and Simple Analytic Representation of the Electron-Gas Correlation Energy," *Phys. Rev. B.*, vol. 45, no. 23, pp. 13244–13249, 1992.
[17] P. E. Blöchl, "Projector Augmented-Wave Method," *Phys. Rev. B.*, vol. 50, no. 24, pp. 17953–17979, 1994.
[18] S. Nachimuthu *et al.*, "A First Principles Study on Boron Doped Graphene Decorated by Ni-Ti-Mg Atoms for Enhanced Hydrogen Storage Performance," *Scient. Rep.*, vol. 5, no. 1, pp. 1–8, 2015.
[19] J. Cervenka and C. F. J. Flipse, "The Role of Defects on the Electronic Structure of A Graphite Surface," *J. Phys. Conf. Ser.*, vol. 61, pp. 190–194, 2007.
[20] J. G. Naeini *et al.*, "Raman scattering from boron-substituted carbon films," *Phys. Rev. B.*, vol. 54, no. 1, p. 144, 1996.
[21] D. Jaeger and J. Patscheider, "A Complete and Self-Consistent Evaluation of XPS Spectra of TiN," *J. Electron Spectro. Related Phenom.*, vol. 185, no. 11, pp. 523–534, 2012.
[22] D. Jaeger and J. Patscheider, Single Crystalline Oxygen-free Titanium Nitride by XPS," *Surf. Sci. Spectra*, vol. 20, no. 1, pp. 1–8, 2017.